

Supplemental Information

Nanoformulation of CCL21 Greatly Increases Its Effectiveness as an Immunotherapy for Neuroblastoma

Brittany J. Poelaert^a, Svetlana Romanova^b, Shelby M. Knoche^a, Madeline T. Olson^a, Bailee H. Sliker^a, Kaitlin Smits^a, Brittney L. Dickey^a, Alexandra E. J. Moffitt-Holida^a, Benjamin T. Goetz^a, Nuzhat Khan^a, Lynette Smith^{c,d}, Hamid Band^{a,c}, Aaron M. Mohs^{b,c,f}, Donald W. Coulter^{c,e}, Tatiana K. Bronich^{b,c}, Joyce C. Solheim^{a,c,f,g,}*

^aEppley Institute for Research in Cancer and Allied Diseases, University of Nebraska Medical Center, Omaha NE 68198

^bDepartment of Pharmaceutical Sciences and Center for Drug Delivery and Nanomedicine, College of Pharmacy, University of Nebraska Medical Center, Omaha NE 68198

^cFred and Pamela Buffett Cancer Center, University of Nebraska Medical Center, Omaha NE 68198

^dDepartment of Biostatistics, University of Nebraska Medical Center, Omaha NE 68198

^eDepartment of Pediatrics, University of Nebraska Medical Center, Omaha NE 68198

^fDepartment of Biochemistry and Molecular Biology, University of Nebraska Medical Center, Omaha NE 68198

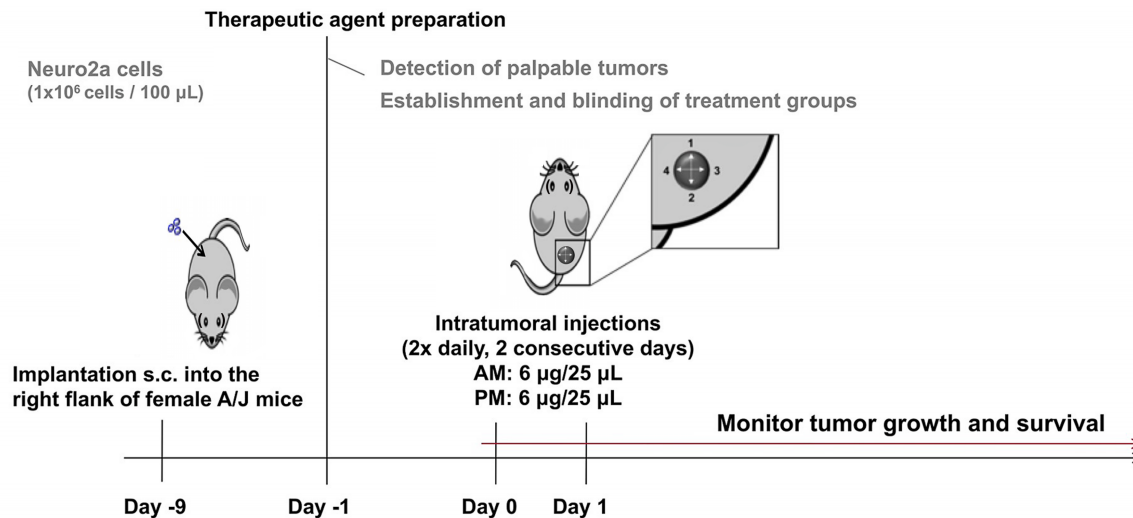


Fig. S1. Strategy for evaluating the therapeutic efficacy of nanoformulated CCL21 in a murine neuroblastoma model. Neuro2a cells (1×10^6 cells/100 μ L) were subcutaneously injected into the lower right flank of female A/J mice and, after palpable tumor formation, the mice were randomly sorted into blinded treatment groups with groups having matched average tumor volumes ($n \geq 6$ mice per group). The mice received intratumoral injections of the respective therapeutic agent twice daily for two consecutive days, delivering 6 μ g CCL21/25 μ L, or 6 μ g of CCL21 in nanoformulation/25 μ L per dose, or an equivalent amount of empty nanoparticles/25 μ L, or the equivalent volume of buffer. To facilitate equal distribution of the injection sites, as well as equal disbursement of the treatments, tumors were visually quartered, and injections were placed as indicated. This strategy was employed for three replicate studies.

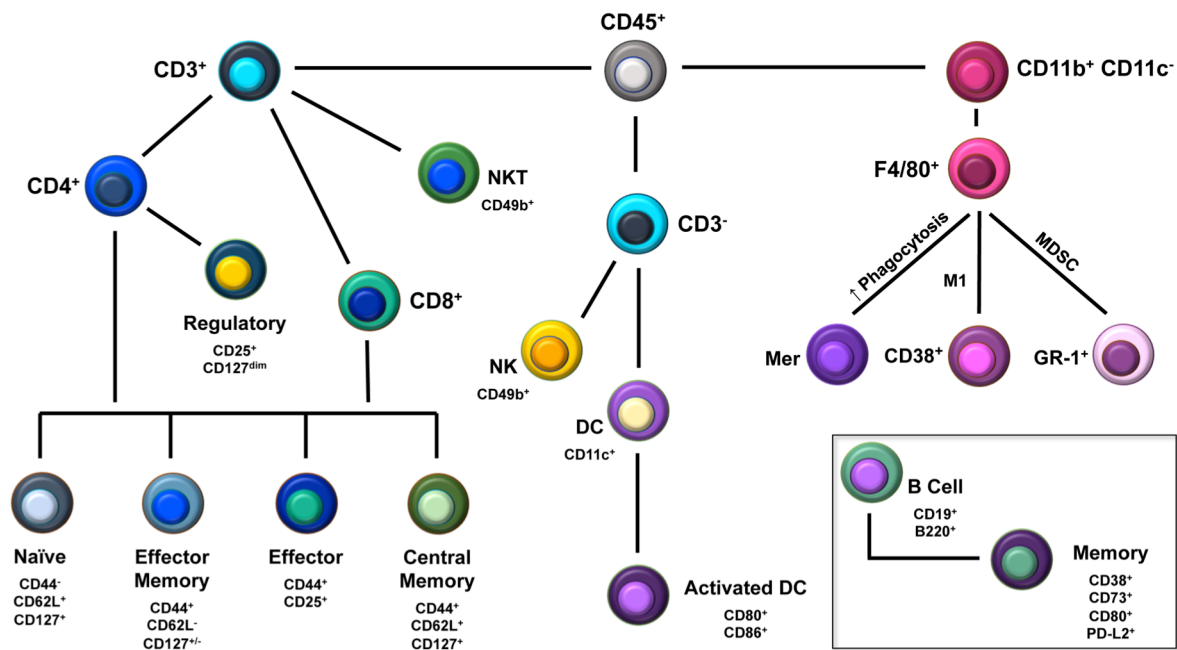


Fig. S2. Schematic of the immunophenotyping strategy that was used to characterize the frequencies of immune cells within treated neuroblastoma tumors.

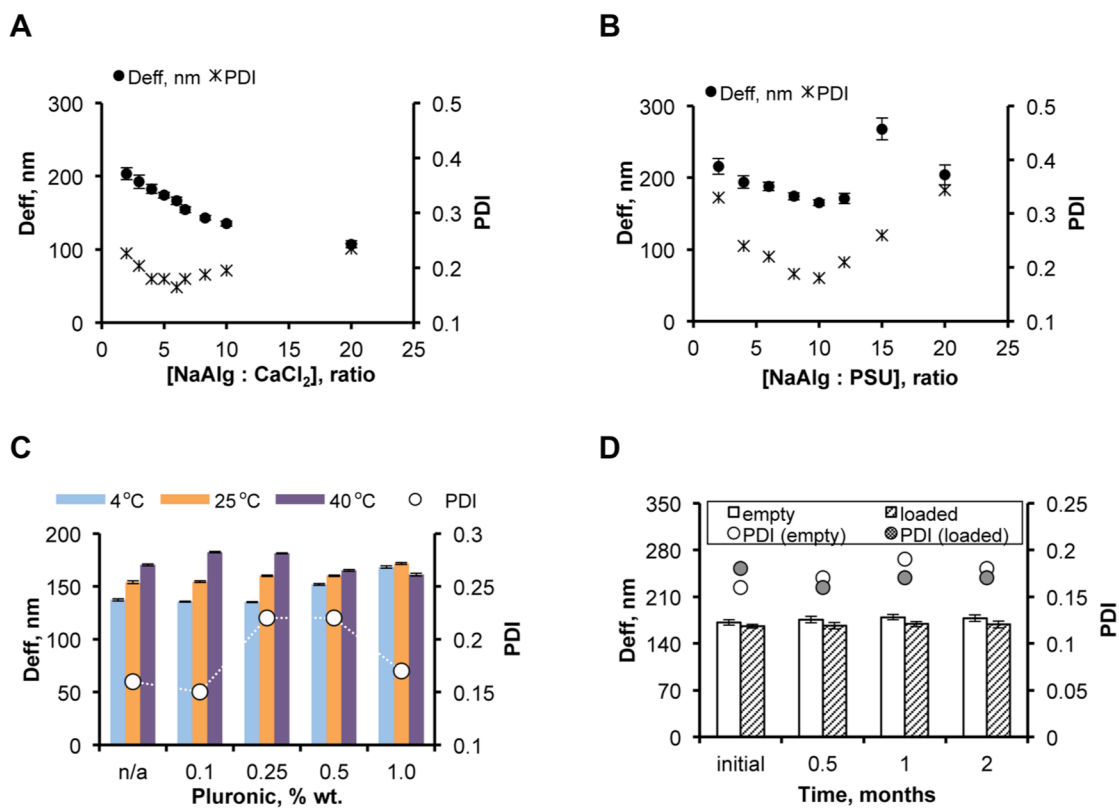


Fig S3. (A) Optimization of the ratio of sodium alginate (NaAlg) to CaCl₂. (B) Optimization of the ratio of NaAlg to protamine sulfate (PSU). (C) Optimization of the percentage of F127 pluronic. (D) Stability of the alginate nanoformulation over a period of time (the nanoformulation was stable for up to 2 months).

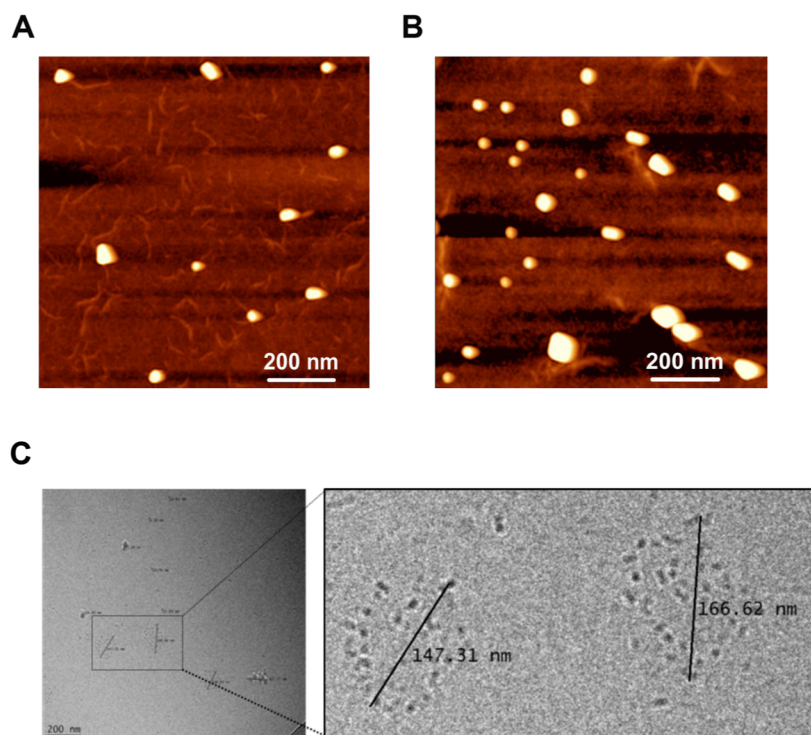


Fig S4. Tapping mode AFM images in air of (A) empty alginate nanoparticles and (B) cytochrome c-loaded alginate nanoparticles. Samples for the AFM imaging were deposited on APS mica from aqueous solutions and dried without washing. In both (A) and (B), the scale bar indicates 200 nm. (C) Cryo-TEM image of cytochrome c-loaded alginate nanoparticles are displayed (scale bar in left panel = 200 nm). The right panel shows a magnified inset from the left panel.

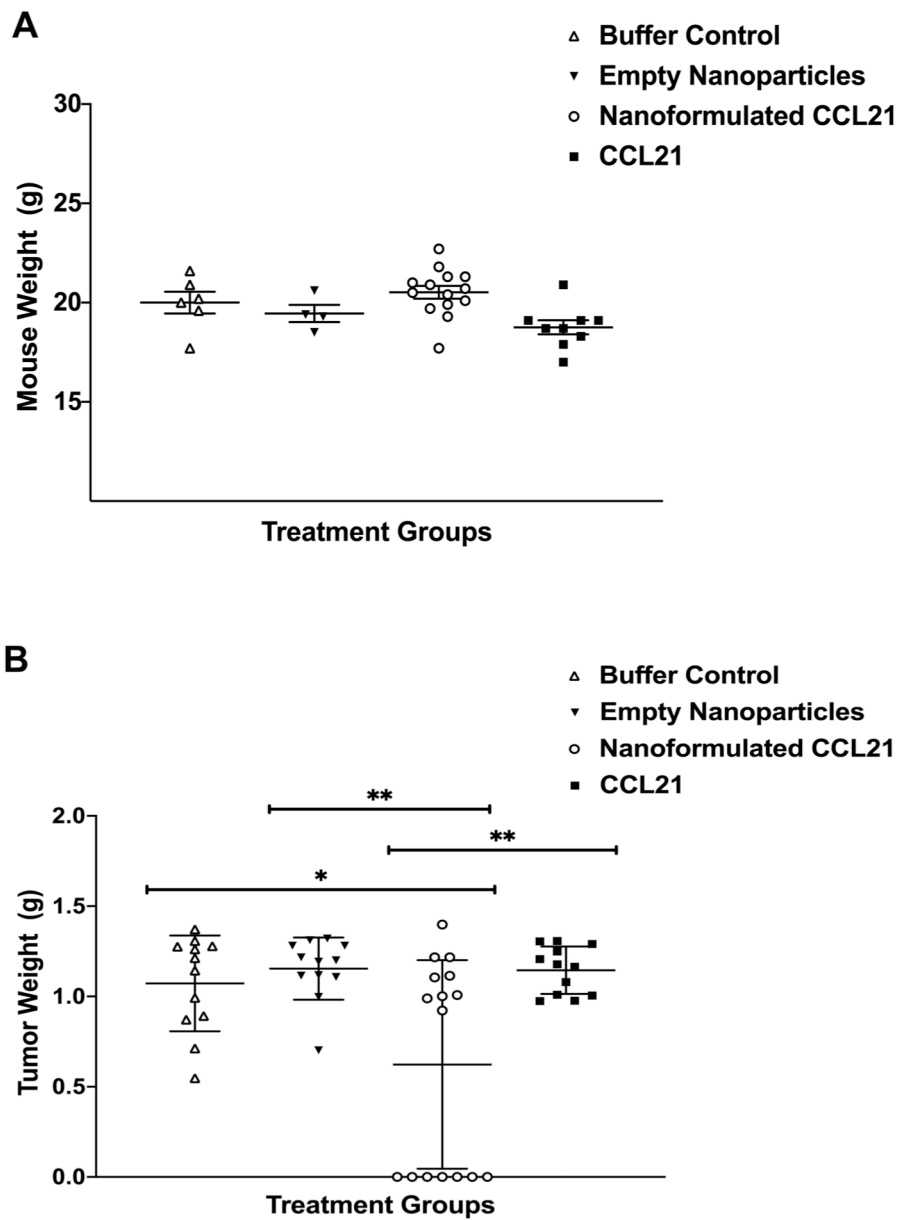


Fig. S5. Average mouse weight was not significantly affected upon intratumoral treatment with nanoformulated CCL21, but average tumor weight was significantly reduced (due to tumor regression in some of the mice). (A) Mouse weights were monitored for the duration of the experiment, and are depicted here until day 8 post-treatment, which was the first day that a mouse reached an endpoint criterion. (B) Primary tumors were resected and weighed at the time of euthanasia of each mouse (once the tumor reached 1000 mm³), and the weights are shown here. The two-tailed t-test was used for comparison of the tumor weights. Nanoformulated CCL21 versus buffer control $p = 0.019$, versus empty nanoparticles $p = 0.0049$, and versus CCL21 $p = 0.0052$. Statistical significance was defined as $p < 0.05^*$ and $p < 0.01^{**}$. For both (A) and (B), the bars represent the mean and SD.

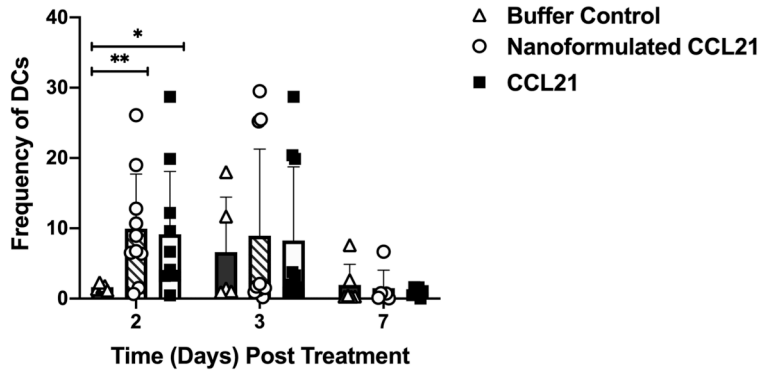
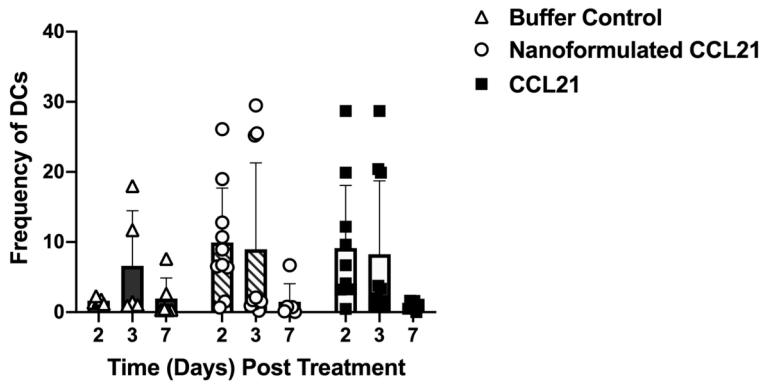
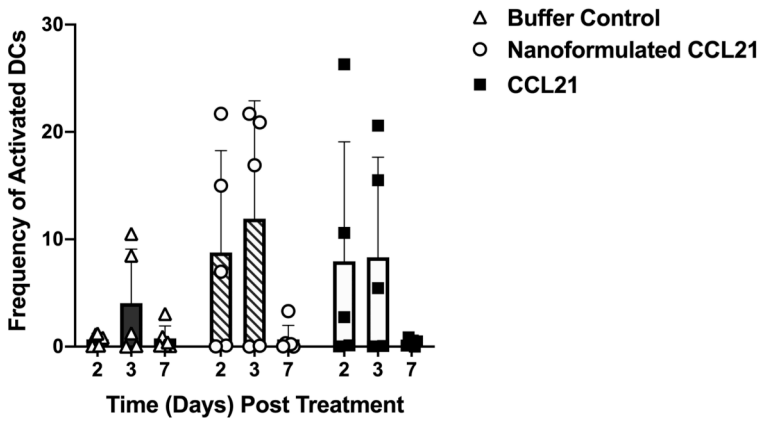
A**B****C**

Fig. S6. Recruitment of DCs into the tumor was increased in the nanoformulated CCL21 and CCL21 treatment groups. (A) Comparisons across treatment groups show a significant increase in the percentage of DCs at day 2 post treatment in the nanoformulated CCL21-treated ($p = 0.0081$) and CCL21-treated ($p = 0.0259$) tumors compared to the control. While not significant, this increase was also observed at day 3 post treatment. (B) Observations within the treatment groups (nanoformulated CCL21 or CCL21) demonstrate a slight decrease from day 2 to day 3 and a larger decrease from day 2 or 3 to day 7. It is also of note that subgroups of high versus low frequencies of DCs were seen in the nanoformulated CCL21 and CCL21 treated groups across time points. (C) Further analysis showed that activated DCs ($CD80^+$ and $CD86^+$) were increased in both treatment groups compared to the control. Gating strategy for DCs: $CD45^+$, $CD3^-$, $CD11c^+$, with an activation state identified as $CD45^+$, $CD3^-$, $CD11c^+$, $CD80^+$, $CD86^+$. Frequency was calculated as $\% \text{ marker} = (\text{number of cells that were marker positive}) / (\text{number of live cells}) \times 100$. Graphical representation of the data depicts the mean frequency overlaid with individual data points for each group. The bars indicate standard deviation. Groups consisted of 5-10 mice per treatment group per time point. Statistical comparisons were made via two-way ANOVA, and p values of ≤ 0.05 were considered to indicate statistical significance.

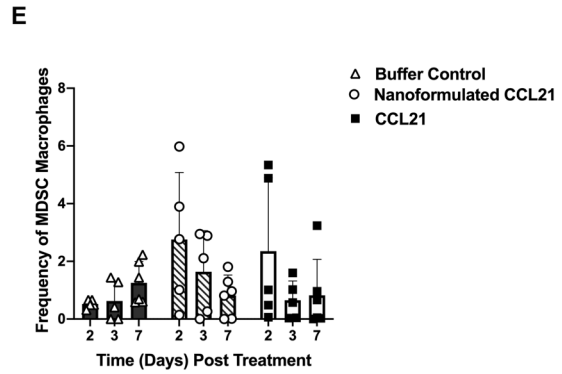
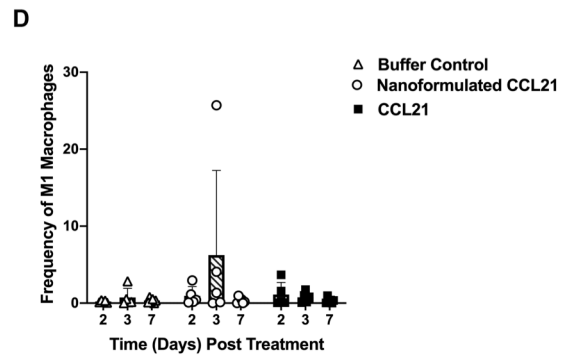
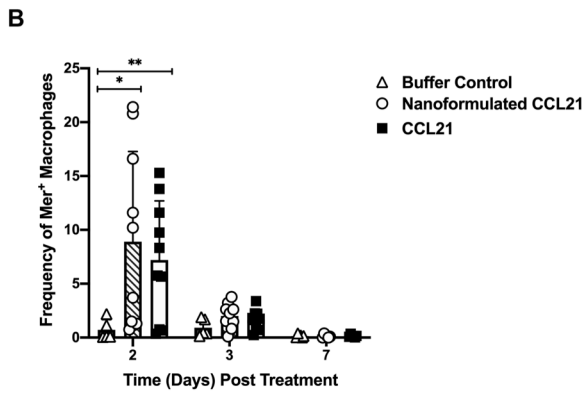
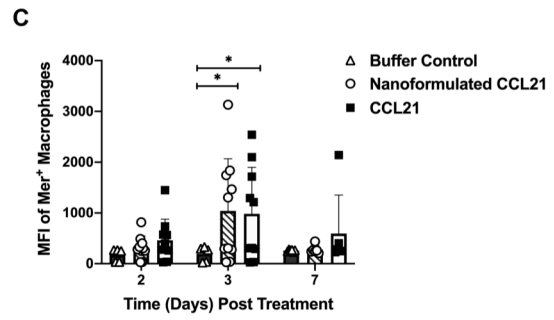
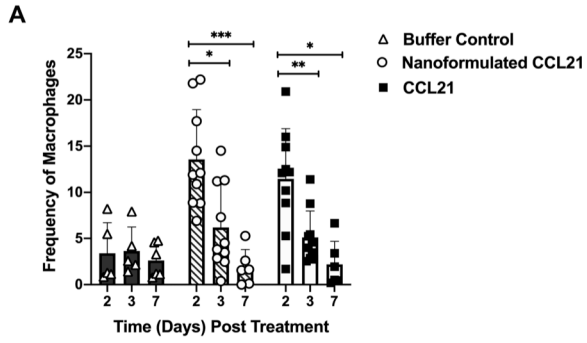


Fig. S7. Nanoformulated CCL21 and CCL21 treatment groups induced changes in the frequency, Mer surface expression levels, and subpopulations of macrophages over time in a manner more varied than the buffer control group. (A) F4/80⁺ macrophages were significantly higher ($p = 0.0007$, $p = 0.0038$) in nanoformulated CCL21-treated and CCL21-treated tumors day 2 post treatment than the tumors treated with buffer control. (B) Analysis of Mer surface expression revealed a peak in the frequencies of Mer⁺ macrophages at day 2 post treatment in the nanoformulated CCL21 and CCL21 treatment groups. These frequencies were significantly higher in the nanoformulated CCL21-treated tumors ($p = 0.0131$) and CCL21-treated tumors ($p = 0.0047$). There was marginally ($p = 0.0564$) higher frequencies of Mer⁺ macrophages at day 3 post treatment in the nanoformulated CCL21 group compared to the buffer control. (C) Subsequently, a significant (nanoformulated CCL21 $p = 0.0282$, CCL21 $p = 0.0240$) peak in the MFI of Mer was observed at day 3 post treatment in either CCL21 modality versus the control. (D) Importantly, nanoformulated CCL21 treatment resulted in a rise in the frequency of M1 macrophages at day 3 post treatment, which was not observed in other groups. (E) Additionally, a stepwise decrease in the percentage of MDSCs appeared to decrease over time in the nanoformulated CCL21-treatment group while the buffer control treatment resulted in increasing percentages of MDSCs within the tumor. Gating strategy for macrophages: CD45⁺, CD11c⁻, CD11b⁺, and F4/80⁺; Mer: CD45⁺, CD11c⁻, CD11b⁺, F4/80⁺, Mer⁺; M1 macrophage: CD45⁺, CD11c⁻, CD11b⁺, F4/80⁺, CD38⁺, GR-1⁻; MDSC macrophage: CD45⁺, CD11c⁻, CD11b⁺, F4/80⁺, CD38⁻, GR-1⁺. Frequency was calculated as % marker = (number of cells that were marker positive) / (number of live cells) x 100. Graphical representation of the data depicts the mean frequency overlaid with individual data points for each group. Statistical comparisons were made via two-way ANOVA. The bars indicate standard deviation. Statistical significance was defined as $p < 0.05^*$, $p < 0.01^{**}$, and $p < 0.001^{***}$. Groups consisted of 5-10 mice per treatment group per time point.

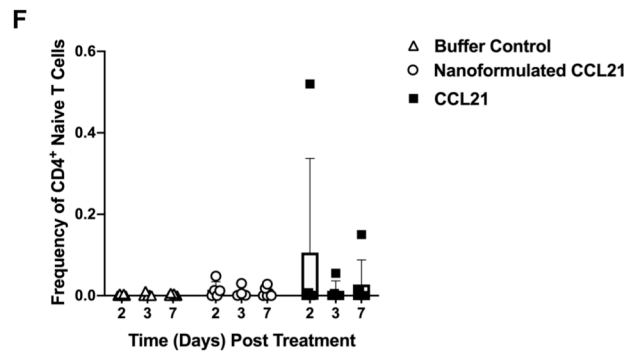
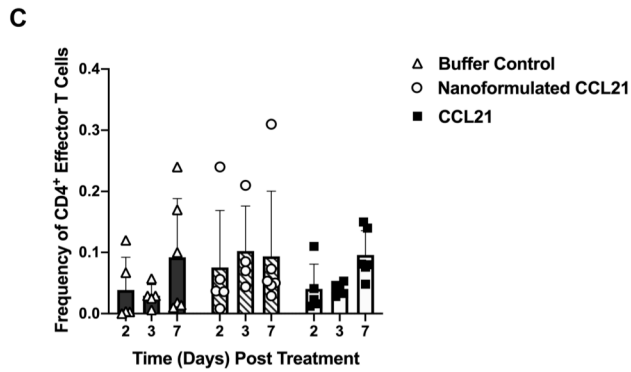
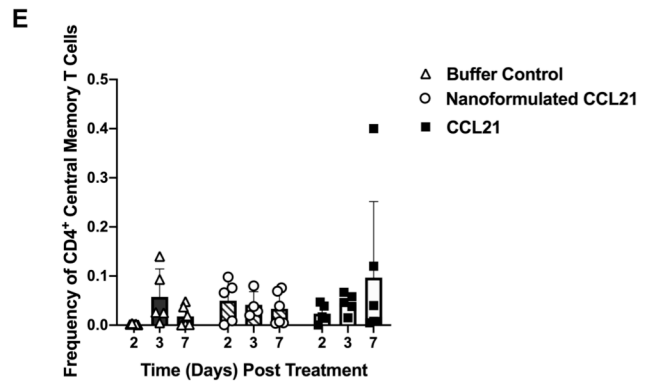
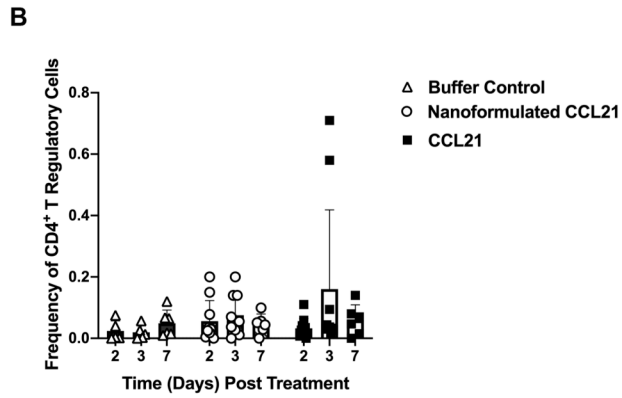
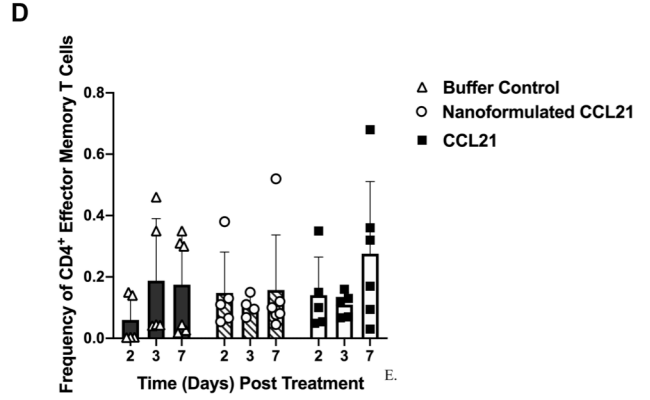
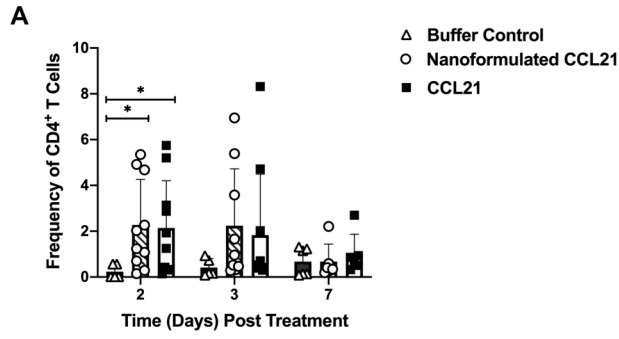


Fig. S8. CD4⁺ T cell populations and subpopulations are differentially modulated following treatment with either nanoformulated CCL21 or CCL21 alone. (A) At day 2 post treatment initiation, CD4⁺ T cell population frequencies were significantly increased in tumors treated with either nanoformulated CCL21 ($p = 0.0105$) or CCL21 alone ($p = 0.0178$) compared to the buffer control. Marginally elevated frequencies of the CD4⁺ T cell population in the CCL21 modalities versus the control, were also observed at day 3 post treatment initiation. (B) CD4⁺ T regulatory cell frequencies appear to decrease from day 2 to day 7 in the nanoformulated CCL21 or CCL21 alone treatment groups. However, the buffer control treatment group appears to have increased frequencies of CD4⁺ T regulatory cells over time. (C) Effector CD4⁺ T cell population frequencies remained constant or were slightly elevated over time across treatment groups. (D) Marginal increases ($p = 0.0665$, $p = 0.0659$) in effector memory CD4⁺ T cell population frequencies was seen in the nanoformulated CCL21-treated or CCL21-treated groups compared to the control-treated group at day 2 post treatment initiation. (E) Central memory CD4⁺ T cell population frequencies were maintained or increased in either CCL21 modality treatment group over time. (F) The frequency of naïve CD4⁺ T cells were increased in the CCL21-treated and nanoformulated CCL21-treated groups compared to the buffer control. Gating strategy for CD4⁺ T cells: CD45⁺, CD3⁺, CD4⁺; CD4⁺ T regulatory cells: CD45⁺, CD3⁺, CD4⁺, CD25⁺, CD127^{dim}; Effector CD4⁺ T Cells: CD45⁺, CD3⁺, CD4⁺, CD25⁺, CD44⁺; Effector Memory CD4⁺ T Cells: CD45⁺, CD3⁺, CD4⁺, CD25⁺, CD44⁺, CD62L⁻, CD127^{+/-}; Central Memory CD4⁺ T Cells: CD45⁺, CD3⁺, CD4⁺, CD25⁺, CD44⁺, CD62L⁺, CD127⁺; Naïve CD4⁺ T Cells: CD45⁺, CD3⁺, CD4⁺, CD25⁻, CD44⁻, CD62L⁻, CD127⁺. Frequency was calculated as % marker = (number of cells that were marker positive) / (number of live cells) x 100. Graphical representation of the data depicts the mean frequency overlaid with individual data points for each group. Statistical comparisons were made via two-way ANOVA. The bars indicate standard deviation. Statistical significance was defined as $p < 0.05^*$. Groups consisted of 5-10 mice per treatment group per time point.

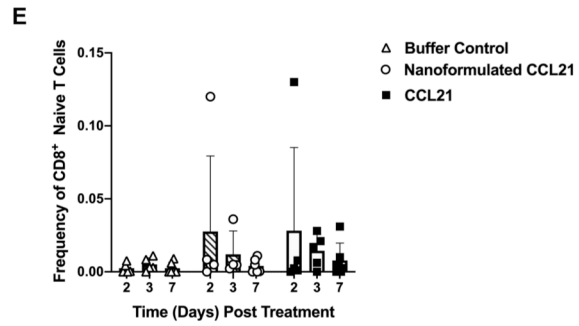
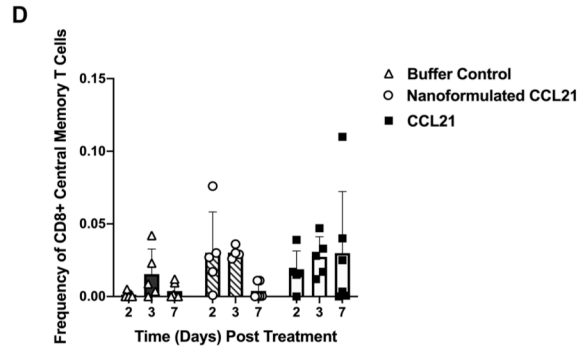
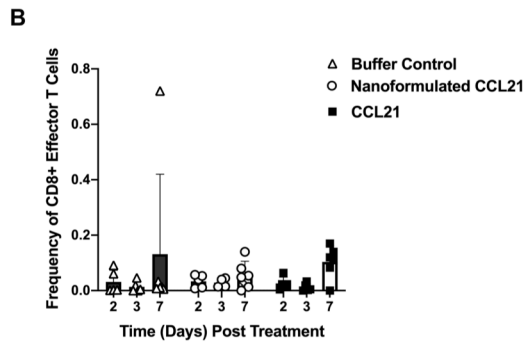
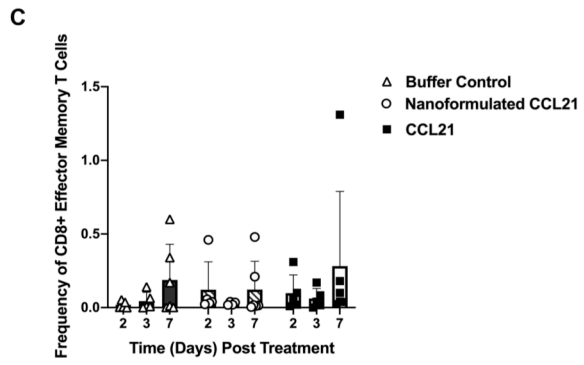
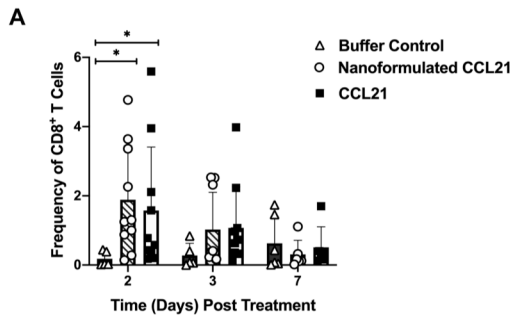


Figure S9. Treatment with nanoformulated CCL21 or CC21 alone alters CD8⁺ T cell populations and subpopulations frequencies within tumors. (A) At day 2 post treatment initiation, CD8⁺ T cell population frequencies were significantly increased in tumors treated with either nanoformulated CCL21 (p = 0.007) or CCL21 alone (p = 0.041) compared to the buffer control. Frequencies of the CD8⁺ T cell populations were marginally elevated in the nanoformulated CCL21-treated (p = 0.084) or CCL21-treated (p = 0.074) versus the control at day 3 post treatment initiation (B) Effector CD8⁺ T cell population frequencies increased over time (disregarding the outlier in the buffer control-treated group day 7). (C) Effector memory CD8⁺ T cell population frequencies demonstrated an increase over time following treatment. (D) Central memory CD8⁺ T cell population frequencies were marginally increased in the nanoformulated CCL21-treated group (p = 0.0825) or the CCL21-treated group (p = 0.0606) at day 2 post treatment. (E) The frequency of naïve CD8⁺ T cell populations were increased in the CCL21-treated and nanoformulated CCL21-treated groups compared to the buffer control over time. Gating strategy for CD8⁺ T cells: CD45⁺, CD3⁺, CD8⁺; Effector CD8⁺ T Cells: CD45⁺, CD3⁺, CD8⁺, CD25⁺, CD44⁺; Effector Memory CD8⁺ T Cells: CD45⁺, CD3⁺, CD8⁺, CD25⁺, CD44⁺, CD62L⁻, CD127^{+/-}; Central Memory CD8⁺ T Cells: CD45⁺, CD3⁺, CD8⁺, CD25⁺, CD44⁺, CD62L⁺, CD127⁺; Naïve CD8⁺ T Cells: CD45⁺, CD3⁺, CD8⁺, CD25⁺, CD44⁻, CD62L⁻, CD127⁺. Frequency was calculated as % marker = (number of cells that were marker positive) / (number of live cells) x 100. Graphical representation of the data depicts the mean frequency overlaid with individual data points for each group. Statistical comparisons were made via two-way ANOVA. The bars indicate standard deviation. Statistical significance was defined as p < 0.05*. Groups consisted of 5-10 mice per treatment group per time point.

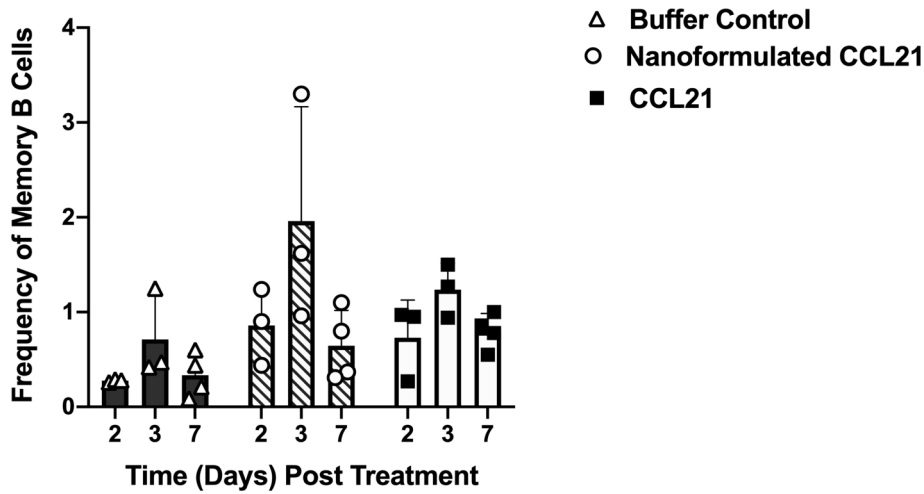
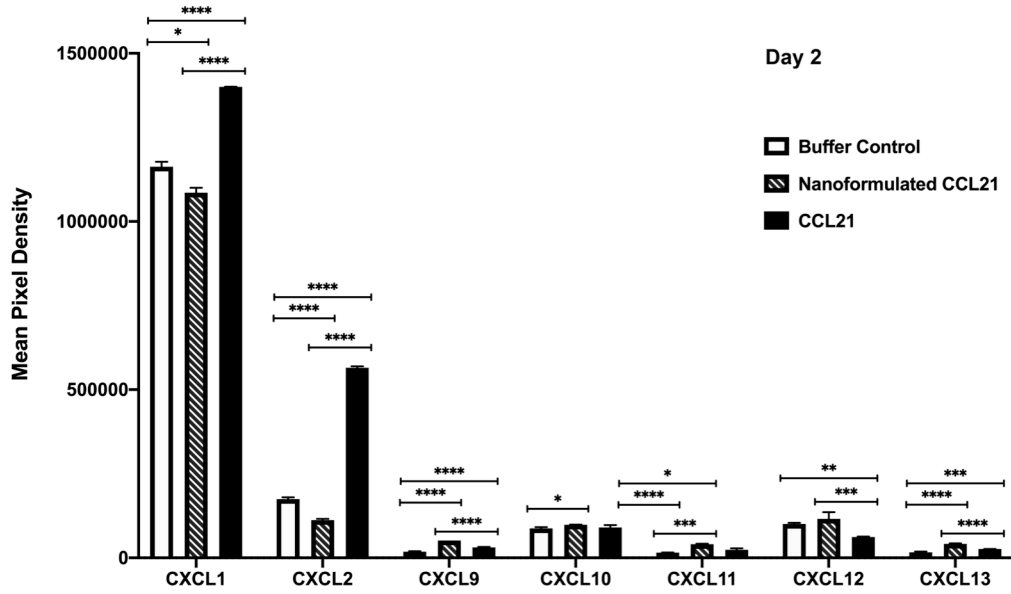
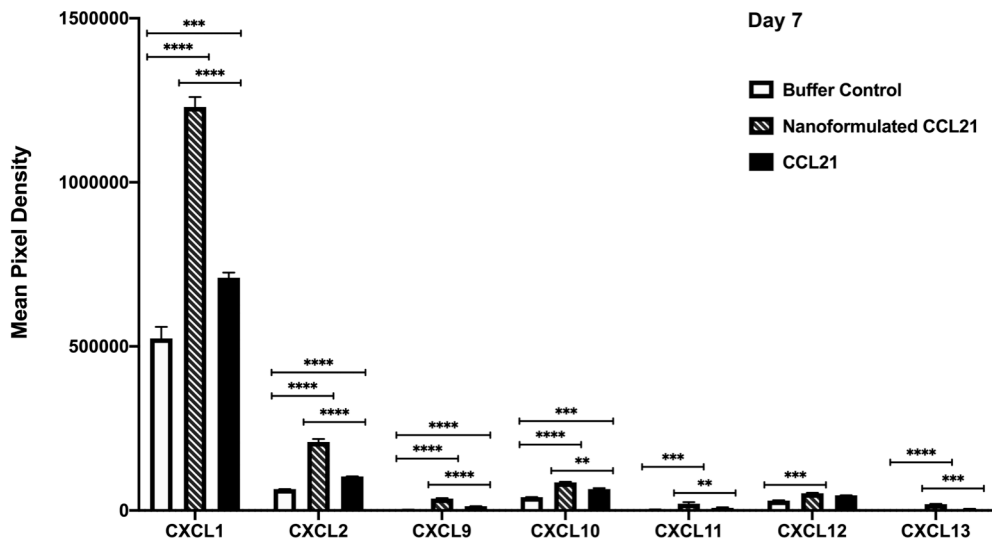
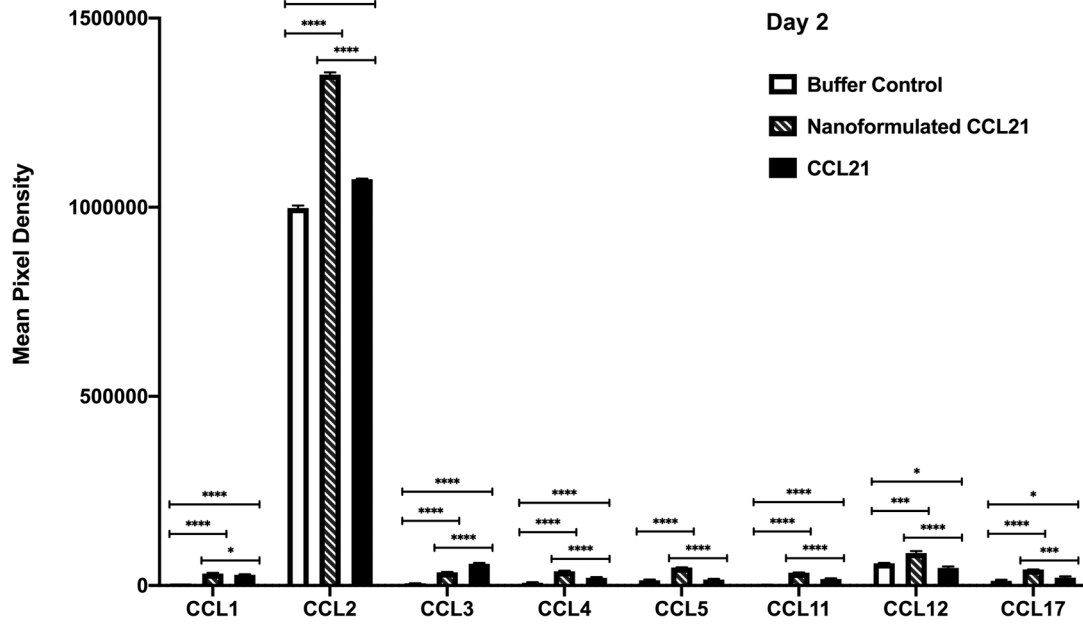


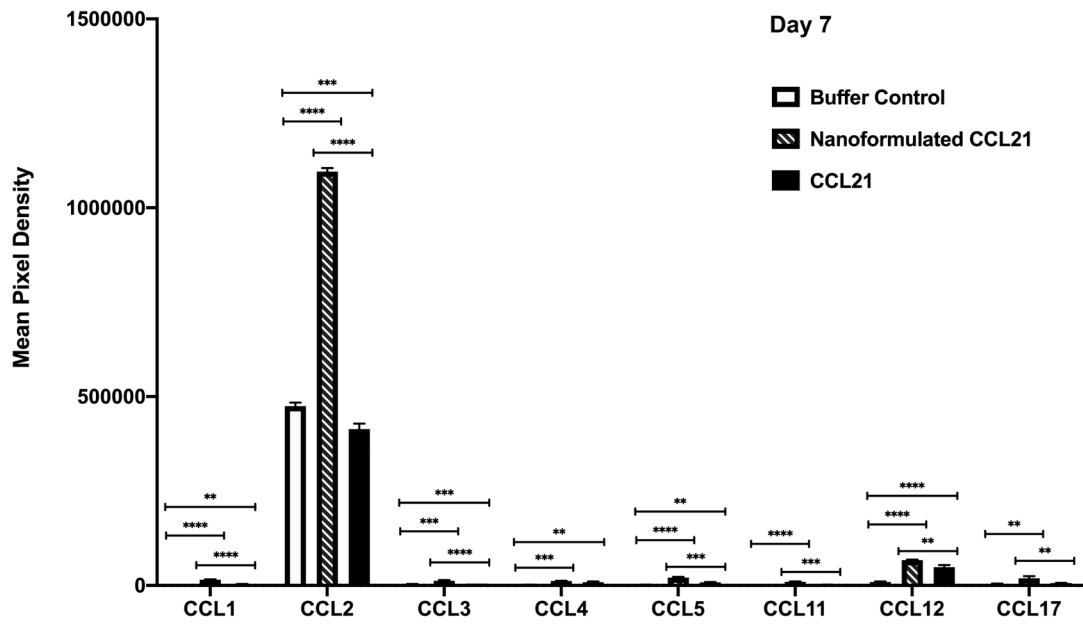
Figure S10. Elevated levels of memory B cells were observed in neuroblastoma tumors treated with either nanoformulated CCL21 or CCL21 in comparison to the control. Gating strategy for memory B cells: B220⁺, CD19⁺, PD-L2⁺, CD73⁺, CD80⁺, and CD38⁺. Frequency was calculated as % marker = (number of cells that were marker positive) / (number of live cells) x 100. Graphical representation of the data depicts the mean frequency overlaid with individual data points for each group. Statistical comparisons were made via two-way ANOVA. The bars indicate standard deviation. Statistical significance was defined as $p < 0.05^*$. Groups consisted of 5-10 mice per treatment group per time point.

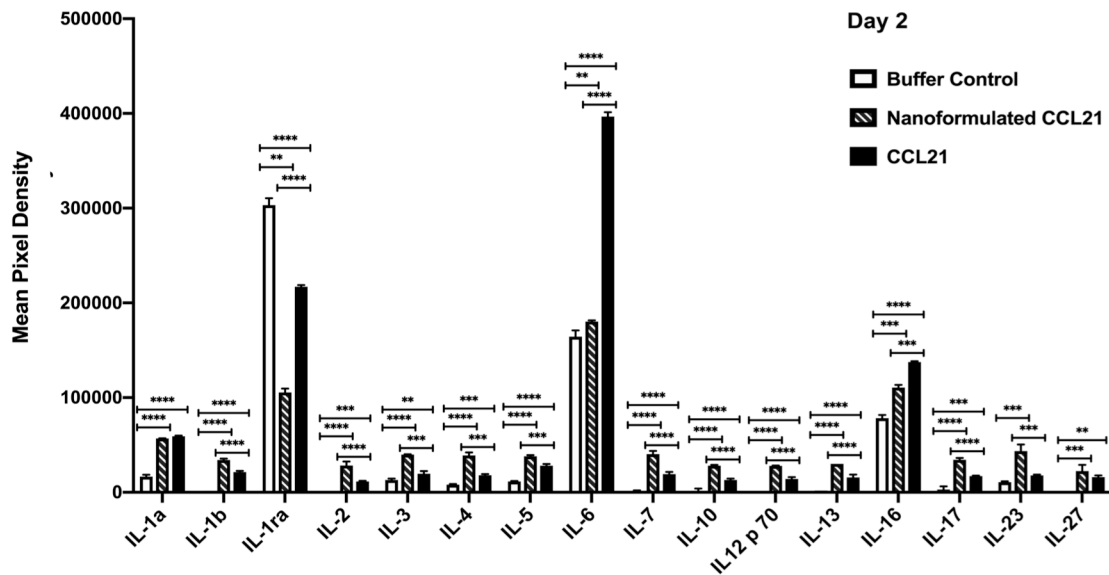
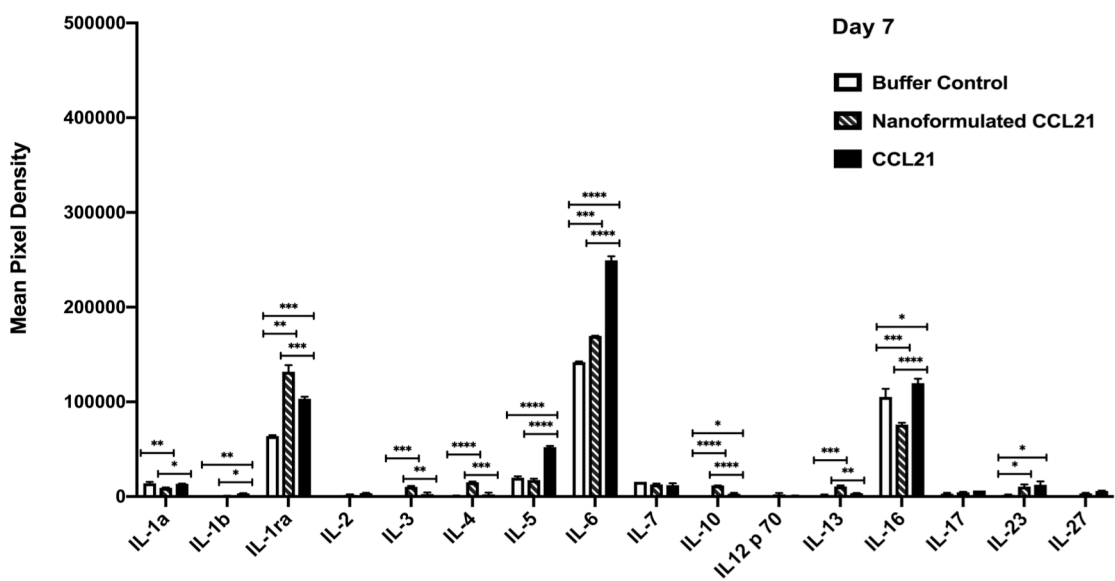
A**B**

C



D



E**F**

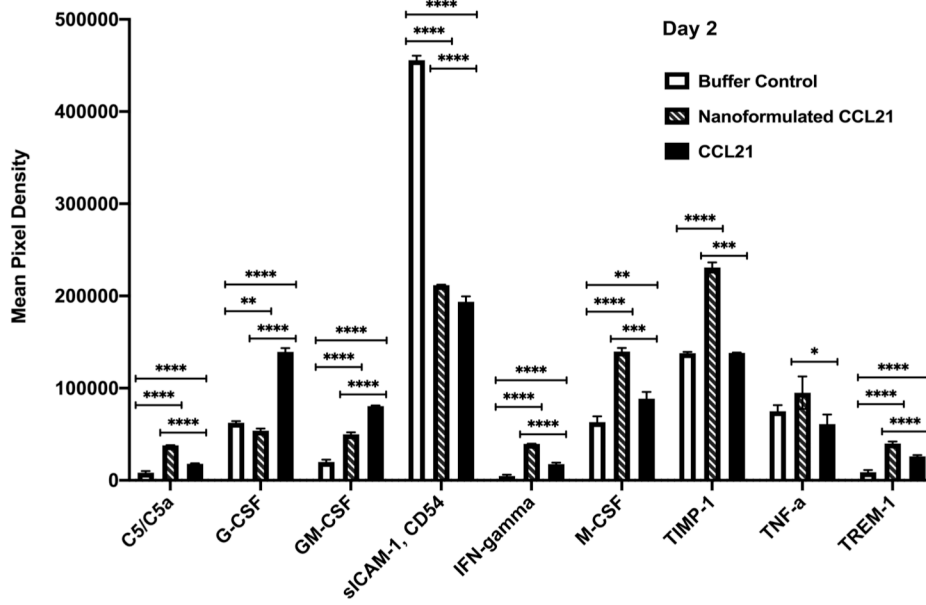
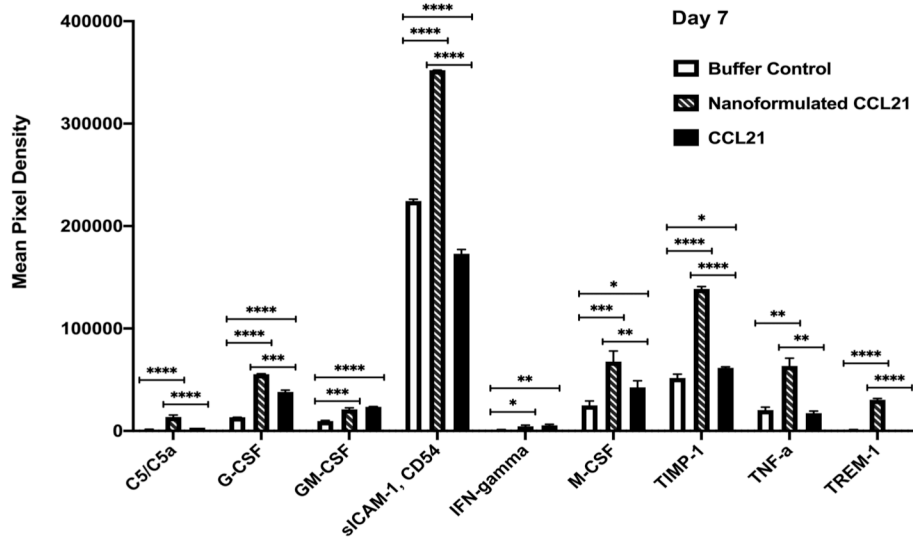
G**H**

Figure S11. Cytokine levels were assessed in tumor supernatants derived from the neuroblastoma tumors of mice euthanized at day 2 or at day 7 post-treatment initiation with nanoformulated CCL21, CCL21 alone, or buffer alone. The Proteome Profiler Mouse Cytokine Array Kit, Panel A (R&D Systems) was used for the analysis. Graphical representation of the data depicts the mean pixel density overlaid with individual data points for each group. Statistical comparisons were made via two-way ANOVA. The bars indicate standard deviation. Statistical significance was defined as $p < 0.05^*$, $p < 0.01^{**}$, $p < 0.001^{***}$, and $p < 0.0001^{****}$. Groups consisted of 5 mice per treatment group per time point.

Table S1. Evaluation of EE and LC

Formulations [Alginate : Cyt c]*	Pluronic	EE, %	LC,%
60:1	-	44.0	1.1
6:1	-	87.2	18.0
60:1	F127, 1%	56.1	1.5
6:1	F127, 1%	99.2	17.7

*The alginate-based nanoparticles were prepared from 4 mL of alginate stock (0.75 mg/ml). Cyt c loading at feeding ratios of 60:1 or 6:1 wt. was carried out either in the presence of Pluronic F127 or without Pluronic F127. The composition ratios of CaCl₂ and protamine sulfate were constant: [Alginate:CaCl₂], 6:1 and [Alginate:Protamine Sulfate], 10:1 wt.

Table S2. Markers used for immunophenotyping

DC and NK cell surface markers used for immunophenotyping

Antibody	Fluorophore	Dilution	Clone	Catalog Nb.
CD45	VioGreen	1:50	REA737	130-110-803
CD3	FITC	1:50	REA641	130-119-758
CD11c	VioBLue	1:50	REA754	130-110-706
MHC Class II	APC	1:50	REA813	130-112-231
CD49b	APC-Vio770	1:10	REA541	120-108-177
CD80	PerCP-Vio700	1:50	REA983	130-116-464
CD86	PE	1:50	REA1190	130-122-129
Live/Dead	UV	1:1000	-	L23105

Macrophage surface markers used for immunophenotyping

Antibody	Fluorophore	Dilution	Clone	Catalog Nb.
CD45	VioGreen	1:50	REA737	130-110-803
F4/80	PerCP-Vio700	1:50	REA126	130-118-327
CD11b	VioBright FITC	1:50	REA592	130-113-243
Mer	APC	1:10	REA477	130-107-479
Ly6C	APC-Vio770	1:50	REA796	130-111-919
CD11c	VioBlue	1:50	REA754	130-110-706
Gr-1	PE-Vio770	1:50	REA810	130-112-308
CD38	PE	1:50	REA616	130-123-571
Live/Dead	UV	1:1000	-	L23105

T cell surface markers used for immunophenotyping

Antibody	Fluorophore	Dilution	Clone	Catalog Nb.
CD45	VioGreen	1:50	REA737	130-110-803
CD3	FITC	1:50	REA641	130-119-758
CD25	PE-Vio770	1:50	REA541	130-123-893
CD4	VioBlue	1:50	REA604	130-119-568
CD8	APC-Vio770	1:50	REA601	130-120-737
CD127	APC	1:50	REA680	120-122-938
CD62L	PerCP-Vio700	1:50	REA828	130-112-651
CD44	PE	1:50	REA664	130-118-566
Live/Dead	UV	1:1000	-	L23105

B cell surface markers used for immunophenotyping

Antibody	Fluorophore	Dilution	Clone	Catalog Nb.
CD45R (B220)	VioBlue	1:50	REA755	130-110-851
CD19	APC-Vio770	1:50	REA749	130-112-038
CD38	FITC	1:50	REA616	130-122-955
CD73	PE-Vio770	1:50	REA778	130-111-519
CD80	PerCP-Vio700	1:50	REA983	130-116-464
CD273 (PD-L2)	APC	1:10	MIH37	130-102-244
Live/Dead	UV	1:1000	-	L23105